Davydov soliton and polarons in molecular chains: Partial Hamiltonian diagonalization

A. M. Clogston
AT&T Bell Laboratories, Murray Hill, New Jersey 07974

H. K. McDowell, Peter Tsai, and Jay Hanssen
Department of Chemistry and Biochemistry, University of Texas at Arlington, Arlington, Texas 76019-0065

(Received 13 May 1998)

The energy of a Davydov soliton from a site-independent or $D2$ wave-function ansatz is obtained in the discrete chain model by using a simulated annealing approach to obtain the envelope of the soliton. Partial diagonalization [A. A. Eremko, Y. B. Gaididei, and A. A. Vakhnenko, Phys. Status Solidi B **127**, 703 (1985)] of the Davydov Hamiltonian allows the soliton to be explicitly displayed in the Hamiltonian. The site-dependent or $D1$ Davydov wave-function ansatz is examined variationally using the simulated annealing approach. This approach leads efficiently to a minimum energy solution in the form of a uniform polaron state as required by translational symmetry. A simple form for the polaron state is displayed. We find no evidence for a minimum energy localized state such as is found from the more constrained $D2$ wave-function ansatz. [S1063-651X(98)15111-5]

PACS number(s): 87.15.−v, 63.20.Ry, 02.70.Rw

I. INTRODUCTION

In 1973 Davydov [1,2] postulated the existence of self-localized states for condensed-matter molecular systems in which high-frequency motions (excitons or molecular vibrations, for example) are nonlinearly coupled to low-frequency (acoustic or optical phonon) motions. Subsequently, Davydov and others refined the initial concepts and additional mechanisms for self-localization were presented [3–5]. The subject received a major boost in 1983 when Careri *et al.* [6,7] produced spectroscopic evidence from infrared and Raman spectroscopy for Davydov-like solitons in acetanilide. This apparent experimental verification was followed by a large body of work, mostly theoretical. An excellent review of this work is available [5].

A variety of Hamiltonians that may or may not reflect true molecular systems have been used to display and presumably to exhibit the Davydov soliton [5]. One of the more widely studied Hamiltonians involves an interaction term that is bilinear in the molecular vibrations and linear in the phonons. The symmetrized version is given by

$$H=\sum_n \left\{\hbar\omega_0\left(c_n^\dagger c_n+\frac{1}{2}\right)-J(c_n^\dagger c_{n+1}+c_{n+1}^\dagger c_n)\right\} + \sum_n \left[\frac{p_n^2}{2M}+\frac{K}{2}(q_{n+1}-q_n)^2\right] + \chi\sum_n c_n^\dagger c_n(q_{n+1}-q_{n-1}), \tag{1}$$

where ω_0 is the frequency of the molecular vibration on each molecule of the chain, J is the dipole-dipole interaction strength between the vibrations, M is the molecular mass, K is the force constant between molecules, χ is the nonlinear coupling constant, q_n and p_n are the position and momentum operators of molecule n, and c_n ($c_n^\dagger$) are the annihilation (creation) operators of the molecular vibration associated with molecule n. The operators c_n and $c_n^\dagger$ obey the usual commutator relations

$$[c_n,c_m^\dagger]=\delta_{nm} \tag{2a}$$

and

$$[c_n,c_m]=[c_n^\dagger,c_m^\dagger]=0. \tag{2b}$$

The Hamiltonian in Eq. (1) does not explicitly display self-localization. As introduced by Eremko, Gaididei, and Vakhnenko [8] and further developed by Cottingham and Schweitzer [9–11] it is possible to transform the Davydov Hamiltonian of Eq. (1) in a formally exact manner into a form that explicitly contains the creation operator for the soliton, self-localized state when the site-independent Davydov $D2$ wave function ansatz is used [5,12]. This transformation, which is called partial diagonalization, has been done previously in the continuum limit [8–11]. In this paper we introduce a simulated annealing procedure that allows us to numerically achieve a similar partial diagonalization for the discrete form in Eq. (6) of Sec. II in the approximation that the chain is finite in length. Using this numerically exact form, we compute elsewhere decay times for the discrete chain as opposed to the continuum case. This finite length approximation is tested by increasing the length of the chain. The simulated annealing algorithm is described in Appendix A. Our approach to partial diagonalization is somewhat different from the previous approaches and we describe this difference in Appendix B.

In Eq. (1) we have used the symmetric form $q_{n+1}-q_{n-1}$ in the nonlinear interaction with the phonons. Although commonly used in studies of the Davydov soliton, it has been criticized as inappropriate for hydrogen-bonded systems such as the alpha helix [13]. We pursue the symmet-

ric form in the present work since it permits comparison with a considerable body of work and we examine other forms in subsequent work.

Other choices for the soliton wave function ansatz have been proposed and they include the site-dependent $D1$ ansatz [14] and a modified $D1$ due to Brown and Ivic [15]. Considerable debate has occurred on the issue of the best structure for this ansatz [15]. The $D1$ ansatz is the most flexible of the extant choices and we examine it herein to determine if it leads to a localized, minimum-energy state. We find that it does not.

This paper is structured as follows: in Sec. II we achieve partial diagonalization of the Hamiltonian in Eq. (1) while defining the creation operator of the $D2$ soliton, self-localized state. We examine in Sec. III both the behavior of the $D2$ soliton energy and the envelope shape of the $D2$ soliton with respect to the Hamiltonian parameters. In Sec. IV we pursue the $D1$ ansatz using simulated annealing. We conclude with summary remarks in Sec. V.

II. PARTIAL DIAGONALIZATION OF THE HAMILTONIAN

We begin by transforming the molecular coordinates to phonon creation and annihilation operators $a_k^\dagger$ and a_k using the standard transformations given by

$$p_n=\sum_{k=-N}^{N}\xi_n^{(k)}\left[\frac{\hbar M\omega_k}{2}\right]^{1/2}(a_k+a_{-k}^\dagger) \tag{3}$$

and

$$q_n=i\sum_{k=-N}^{N}\xi_n^{(k)}\left[\frac{\hbar}{2M\omega_k}\right]^{1/2}(a_k-a_{-k}^\dagger), \tag{4}$$

with

$$\xi_n^{(k)}=\frac{\exp[2\pi i(kn)/(2N+1)]}{\sqrt{2N+1}}. \tag{5}$$

The constant N specifies a chain of length $2N+1$ with sites labeled $-N$ to N and N is taken to be finite but large enough so that increasing N has no effect on calculated results. Substituting Eqs. (3) and (4) into Eq. (1) yields

$$\begin{aligned}H=&\sum_n\left\{\hbar\omega_0\left(c_n^\dagger c_n+\frac{1}{2}\right)-J(c_n^\dagger c_{n+1}+c_{n+1}^\dagger c_n)\right\}\\&+\sum_{k=-N}^{N}\hbar\omega_k(a_k^\dagger a_k+\tfrac{1}{2})\\&-\sum_{k=-N}^{N}\sum_{n=-N}^{N}c_n^\dagger c_n(\chi_k^{(n)}a_k+\chi_k^{(n)*}a_k^\dagger),\end{aligned} \tag{6}$$

where

$$\overline{\chi}=\chi\left(\frac{\hbar}{2M\omega_a}\right)^{1/2}, \tag{7}$$

$$\omega_k=\omega_a\left|\sin\frac{\pi k}{2N+1}\right|, \tag{8}$$

$$\omega_a=2\sqrt{K/M}, \tag{9}$$

$$\sigma_k=4\overline{\chi}\ \mathrm{sgn}\ k\ \cos\left(\frac{\pi k}{2N+1}\right)\left(\frac{|\sin[\pi k/(2N+1)]|}{2N+1}\right)^{1/2}, \tag{10}$$

and

$$\chi_k^{(n)}=\sigma_k\exp\left(2\pi i\ \frac{kn}{2N+1}\right). \tag{11}$$

The function sgn k produces the sign of k. The above conventional analysis implies a cyclic chain since from Eqs. (4) and (5) we find $q_{N+1}=q_{-N}$. We also introduce the parameter

$$\eta=\frac{2\overline{\chi}^2}{\hbar^2\omega_a}=(2N+1)\ \frac{\sigma_k^2}{8\hbar^2\omega_k}\bigg|_{k=0} \tag{12}$$

for later use. The Hamiltonian in Eq. (6) is the starting point for our Davydov soliton analysis.

We define a $D2$ soliton creation operator by

$$A_s^\dagger=\sum_m\ a_{ms}c_m^\dagger\exp\left[\sum_k\ (s_k a_k-s_k^* a_k^\dagger)\right], \tag{13}$$

where s_k and a_{ms} are parameters to be determined by energy minimization. This choice for the creation operator is due to Davydov [12] and is known as the $D2$ ansatz [5]. It provides a coherent state structure for the phonons when time dependence is included. In the present work we are only interested in the static structure of the $D2$ soliton in terms of energy minimization of the Hamiltonian expectation value for the variational state created by the operation of the creation operator in Eq. (13) on the vacuum. Elsewhere, we include the time dynamics of the second quantized operators in the Heisenberg sense to examine issues of the lifetime of the $D2$ soliton.

Following Eremko, Gaididei, and Vakhnenko [8] and Cottingham and Schweitzer [9–11], we want to carry out a partial diagonalization of Eq. (6) such that the soliton operator in Eq. (13) appears naturally. We review their approach in Appendix B. To accomplish this task, we use the unitary transformation given by

$$U^\dagger=\exp\left[\sum_m\ c_m^\dagger c_m\left(\sum_k\ (s_k^* a_k^\dagger-s_k a_k)\right)\right], \tag{14}$$

with

$$D_m=Uc_mU^\dagger=c_m\exp\left[\sum_k\ (s_k^* a_k^\dagger-s_k a_k)\right] \tag{15}$$

and

$$B_k=Ua_kU^\dagger=a_k+s_k^*\sum_m\ c_m^\dagger c_m \tag{16}$$

to obtain

$$H=\sum_n \{\hbar\omega_0 D_n^\dagger D_n - J(D_n^\dagger D_{n+1}+D_{n+1}^\dagger D_n)\}$$
$$+\sum_k \hbar\omega_k B_k^\dagger B_k + \left(\sum_k \hbar\omega_k s_k^* s_k\right)\sum_{mn} D_m^\dagger D_m D_n^\dagger D_n$$
$$+\sum_{kn} (\chi_k^{(n)} s_k^* + \chi_k^{(n)*} s_k)\sum_m D_m^\dagger D_m D_n^\dagger D_n$$
$$-\sum_{kn} \{(\hbar\omega_k s_k + \chi_k^{(n)}) B_k D_n^\dagger D_n$$
$$+(\hbar\omega_k s_k^* + \chi_k^{(n)*}) B_k^\dagger D_n^\dagger D_n\}. \quad (17)$$

Unnecessary zero-point energy terms have been dropped. From Eq. (2) and the unitary transformation in Eq. (15), it is clear that D_n and $D_n^\dagger$ obey the usual commutator relations. Noting that

$$D_m^\dagger D_m D_n^\dagger D_n = D_m^\dagger D_n^\dagger D_m D_n + \delta_{nm} D_n^\dagger D_n, \quad (18)$$

we have

$$H=H_0+\sum_k \hbar\omega_k B_k^\dagger B_k - \sum_{kn} \{(\hbar\omega_k s_k + \chi_k^{(n)}) B_k D_n^\dagger D_n$$
$$+(\hbar\omega_k s_k^* + \chi_k^{(n)*}) B_k^\dagger D_n^\dagger D_n\}$$
$$+\sum_{kn} (\hbar\omega_k s_k^* s_k + \chi_k^{(n)} s_k^* + \chi_k^{(n)*} s_k)\sum_m D_m^\dagger D_n^\dagger D_m D_n, \quad (19)$$

where H_0 is defined by

$$H_0=\sum_n \{\varepsilon_n D_n^\dagger D_n - J(D_n^\dagger D_{n+1}+D_{n+1}^\dagger D_n)\} \quad (20)$$

and

$$\varepsilon_n=\hbar\omega_0+\sum_k (\hbar\omega_k s_k^* s_k + \chi_k^{(n)} s_k^* + \chi_k^{(n)*} s_k). \quad (21)$$

Note that H_0 is tridiagonal with ε_n and J real. We use cyclic boundary conditions on the chain such that $D_{N+1}=D_{-N}$.

Following Eremko, Gaididei, and Vakhnenko [8], we now proceed to diagonalize the Hamiltonian H_0 by a unitary transformation whose elements are $a_{n\nu}$ with

$$D_n=\sum_\nu a_{n\nu} A_\nu \quad (22)$$

and

$$\sum_\nu a_{n\nu} a_{m\nu}^* = \delta_{nm}, \quad \sum_n a_{n\nu} a_{n\mu}^* = \delta_{\nu\mu}. \quad (23)$$

Note that $a_{n\nu}$ is a square matrix of dimension $2N+1$. If the transformation in Eq. (22) is applied to Eq. (20), we obtain

$$H_0=\sum_\nu E_\nu A_\nu^\dagger A_\nu \quad (24)$$

by requiring

$$\sum_n \{\varepsilon_n a_{n\mu}^* a_{n\nu} - J(a_{n\mu}^* a_{n+1,\nu} + a_{n+1,\mu}^* a_{n\nu})\} = E_\nu \delta_{\mu\nu}. \quad (25)$$

We next multiply by $a_{m\mu}$ and sum over μ to obtain

$$\varepsilon_m a_{m\nu} - J(a_{m+1,\nu} + a_{m-1,\nu}) = E_\nu a_{m\nu}. \quad (26)$$

It is obvious from Eq. (26) that $a_{m\nu}$ can be taken real without loss of generality.

We now determine the parameter s_k by minimizing the energy of one state, which we designate the soliton state with $\nu=s$. From Eq. (25) we have

$$E_s=\sum_n \{\varepsilon_n a_{ns}^2 - 2J a_{ns} a_{n+1,s}\}. \quad (27)$$

We require

$$\frac{\partial E_s}{\partial s_k^*}=\sum_n a_{ns}^2 \frac{\partial \varepsilon_n}{\partial s_k^*}=0 \quad (28)$$

and using Eq. (21) obtain

$$s_k=-\frac{\Sigma_n a_{ns}^2 \chi_k^{(n)}}{\hbar\omega_k}. \quad (29)$$

Placing this result in Eq. (21), we find

$$\varepsilon_n=\hbar\omega_0+\sum_{jm} a_{js}^2 a_{ms}^2 \sum_k \frac{\chi_k^{(j)*}\chi_k^{(m)}}{\hbar\omega_k}$$
$$-\sum_m a_{ms}^2 \sum_k \frac{(\chi_k^{(n)*}\chi_k^{(m)} + \chi_k^{(n)}\chi_k^{(m)*})}{\hbar\omega_k}, \quad (30)$$

which, using Eqs. (10), (11), and (12), becomes

$$\varepsilon_n=\hbar\omega_0+2\hbar\eta\left\{\sum_m [2a_{ms}^4 + a_{ms}^2(a_{m+1,s}^2 + a_{m-1,s}^2)]\right.$$
$$\left.-2[2a_{ns}^2 + a_{n+1,s}^2 + a_{n-1,s}^2]\right\}. \quad (31)$$

If a_{ms} is either symmetric or antisymmetric about $n=s$, ε_n is symmetric about $n=s$.

Inserting the expression for ε_n given by Eq. (31) into Eq. (27), we obtain

$$E_s=\hbar\omega_0-2\hbar\eta\sum_n a_{ns}^2(2a_{ns}^2 + a_{n+1,s}^2 + a_{n-1,s}^2)$$
$$-2J\sum_n a_{ns} a_{n+1,s}. \quad (32)$$

Equation (32) is the standard equation, which must be minimized to obtain the excitation envelope for the $D2$ Davydov soliton [16],

In Appendix A we describe a simulated annealing computer code, which can be used to obtain numerical values for the coefficients a_{ns}. Once the soliton envelope is computed,

the Hamiltonian H_0 is completely defined since the envelope parameters a_{ns} determine s_k in Eq. (29), which in turn determine ε_n in Eq. (31). We can then diagonalize the tridiagonal matrix represented in Eq. (25) using the Jacobi algorithm [17]. Consistency requires the lowest eigenvalue to be E_s and the eigencoefficients a_{ns} to be the same as those obtained from the simulated annealing minimization. This indeed proves to be the case.

Having diagonalized H_0, we transform the full Hamiltonian in Eq. (19) using Eq. (22) and obtain

$$H=\sum_{\nu} E_{\nu}A_{\nu}^{\dagger}A_{\nu}+\hbar\sum_{k} \omega_k B_k^{\dagger}B_k$$

$$+\hbar\sum_{k\mu\nu}[R(k,\mu,\nu)B_k+R(k,\mu,\nu)^*B_k^{\dagger}]A_{\mu}^{\dagger}A_{\nu}$$

$$+\sum_{\mu\nu} G_{\mu\nu}\sum_{\lambda} A_{\lambda}^{\dagger}A_{\mu}^{\dagger}A_{\lambda}A_{\nu}, \tag{33}$$

where

$$R(k,\mu,\nu)=\frac{1}{\hbar}\sum_{n} \chi_k^{(n)}(a_{ns}^2\delta_{\mu\nu}-a_{n\mu}a_{n\nu}) \tag{34}$$

and

$$G_{\mu\nu}=4\hbar\eta\sum_{n} a_{n\mu}a_{n\nu}\Bigg[\sum_{m} (a_{ms}^4+a_{ms}^2a_{m+1,s}^2)$$

$$-a_{n+1,s}^2-2a_{n,s}^2-a_{n-1,s}^2\Bigg]. \tag{35}$$

Note that $R(k,s,s)=0$. The partially diagonalized, discrete chain Hamiltonian in Eq. (33) is the basis for the results described herein. Although similar in spirit to previous partially diagonalized Hamiltonians in the continuum approximation [8–11], it differs in that fully dressed operators in Eqs. (15) and (16) are used which leads to the multiexcitation term involving $G_{\mu\nu}$. It is important to understand that the Hamiltonian in Eq. (33) is equivalent to the original Davydov Hamiltonian in Eq. (1) having been obtained by unitary transformations of the second-quantized operators.

III. COMPUTATIONAL RESULTS FOR $D2$ SOLITON

We next survey the results obtained from the diagonalization of H_0 for various choices of the underlying parameters $\hbar\omega_0$, $\hbar\omega_a$, $\overline{\chi}$, and J. Note that the diagonalization process does not depend on temperature. As discussed in Appendix A, we arrange for the soliton to be centered about site 0. We begin by examining the energy values E_{ν}. We choose two classes of parameter values: one class is exemplified by set 5 (see Table III) and is given by $\hbar\omega_0=1665\ \mathrm{cm}^{-1}$, $\hbar\omega_a=100\ \mathrm{cm}^{-1}$, $\overline{\chi}=10\ \mathrm{cm}^{-1}$, and $J=1\ \mathrm{cm}^{-1}$; the other class is exemplified by set 14 where $\hbar\omega_0=1665\ \mathrm{cm}^{-1}$, $\hbar\omega_a=88\ \mathrm{cm}^{-1}$, $\overline{\chi}=10\ \mathrm{cm}^{-1}$, and $J=7.8\ \mathrm{cm}^{-1}$. The first class (set 5) is the small J regime while the second class (set 14) represents the range of values described as the normal set for matching alpha-helix parameters [5]. In Figs. 1 and 2 we display the $D2$ oscillator energy values E_{ν} for set 14 and set 5, respectively, and in Table I the envelope amplitudes (where they are symmetric about site 0, we display only half the envelope) for the ground state or lowest energy oscillator. It is clear from these results that a localized excitation spanning 10 to 20 sites exists for the lowest energy of H_0. The envelope for set 5 is more localized and reflects the smaller value for J. Furthermore, we see for set 5 that an additional pair of energy values drop below the energy band. Their amplitudes $a_{n\nu}$ are also given in Table I and we see that they are also localized about site 0.

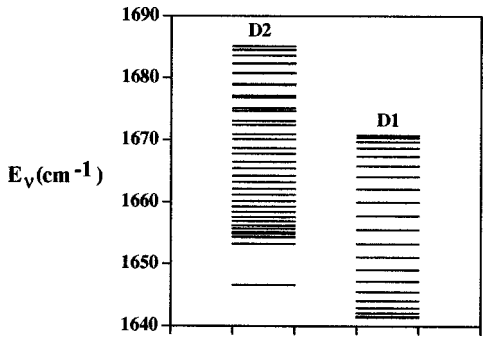

FIG. 1. Comparison of $D1$ and $D2$ energy spectra for H_0 using set 14 parameters.

To understand the behavior of the oscillator energies in set 5, we examine the limit $J=0$. In this limit we find from Eq. (20) that H_0 is already diagonal and thus the transformation matrix $a_{n\nu}$ is the unit matrix and $E_n=\varepsilon_n$ with ε_n defined in Eq. (21) and computed in Eq. (31) in terms of a_{ns}. In this special case of $J=0$, the energies E_n are site specific; that is, energy E_n is assigned to the oscillator at site n. Since $n=0$ is chosen as the center of the soliton, we have $a_{ms}=\delta_{m0}$ and we find for $n=0$ that

$$E_0=\varepsilon_0=\hbar\omega_0-4\hbar\eta, \tag{36}$$

which has a value of 1657 cm^{-1} for set 5. For the two cases $n=+1$ and $n=-1$, we obtain

$$E_{+1}=E_{-1}=\hbar\omega_0, \tag{37}$$

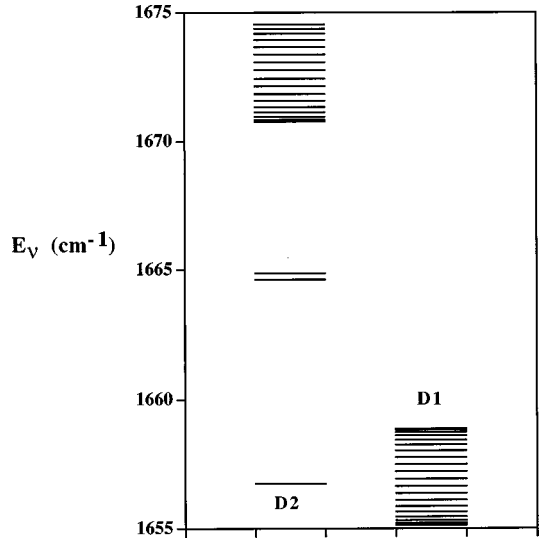

FIG. 2. Comparison of $D1$ and $D2$ energy spectrum for H_0 using set 5 parameters.

TABLE I. Envelope amplitudes a_{ns} for localized states.

Set 14		Set 5					
Ground state		Ground state		Localized pair			
n	a_{ns}	n	a_{ns}	n	$a_{n\nu}$	n	$a_{n\nu}$
0	0.668 691	0	0.984 450	−5	0.000	−5	0.000
1	0.470 881	1	0.123 966	−4	0.001	−4	0.002
1	0.214 606	2	0.007 837	−3	0.011	−3	0.012
3	0.085 634	3	0.000 492	−2	0.089	−2	0.091
4	0.033 343	4	0.000 031	−1	0.701	−1	0.690
5	0.012 933	5	0.000 002	0	0.000	0	−0.175
6	0.005 013			1	−0.701	1	0.690
7	0.001 943			2	−0.089	2	0.091
8	0.000 753			3	−0.011	3	0.012
9	0.000 292			4	−0.001	4	0.002
10	0.000 113			5	−0.000	5	0.000
11	0.000 044						
12	0.000 017						
13	0.000 006						
14	0.000 002						

which has the value 1665 cm^{-1} for set 5. Finally, we have for the remaining energies that

$$E_n=\hbar\omega_0+4\hbar\eta, \tag{38}$$

which has the value 1673 cm^{-1} for set 5. Thus, we predict that the spectrum of the oscillator energies in H_0 at small J will manifest a single low energy value, an intermediate pair of nearly degenerate values, and a band of values as is seen in Fig. 2. To show that the set 5 results extrapolate to the three energy values predicted above, we present in Table II a sequence of calculations in which J is varied while other parameters are maintained at their set 5 values. For the band of energy values we report only the lower and upper band energies from the finite dimensional matrix diagonalization. As J approaches zero, the limiting values are clearly approached.

We next compare the energy of the localized state E_S as found in Table III with the continuum model energy E_{SC}. Note first that a_{ns} and E_S obtained by minimizing Eq. (32) depends only on ω_0, η, and J. This is, of course, true also of E_{SC} given by [9]

$$E_{sc}=\hbar\omega_0-2J-\frac{16}{3}\frac{\hbar^2\eta^2}{J}. \tag{39}$$

A plot comparing E_S and E_{SC} is shown in Fig. 3 for various values of J and η with $\hbar\omega_0=1665$ cm^{-1}. For each value of J the plots show a locus of pairs of values of E_{SC} and E_S increasing monotonically towards the diagonal as η decreases. The obvious reason for this is that the soliton state broadens as η decreases so that the discrete and continuum values of the soliton energy converge. This behavior can be understood in more detail by examining the column labeled ''n'' in Table III. This column contains the value of n for the envelope a_{ns} of the localized state where a_{ns} first drops below 10^{-4} and is thus a measure of the width of the localized state. We find for $J=7.8$ that n is larger, which indicates a localized state spread over more sites. As argued by others [5], such a state is expected to more closely follow the continuum model. For a separate check on this contention, we compare in Table IV our calculated envelope with the continuum model envelope given by [9,18]

$$a_{ns}^c=\left(\frac{2\hbar\eta}{J}\right)^{1/2}\operatorname{sech}\left(\frac{4\hbar\eta}{J}\,n\right). \tag{40}$$

Set 9 of Table III is the most diffuse local state and we find from Table IV that the discrete chain envelope is similar to the continuum model. For set 5, a very narrow localized state, the continuum model breaks down. On the other hand, the parameter $J/\hbar\eta$ in Eq. (40) is clearly a measure of the

TABLE II. Behavior of energy levels for small J. Energy units are cm^{-1}.

	Ground	Pair		Band	
J		Lower	Upper	Lower	Upper
0[a]	1657.00	1665.00	1665.00	1673.00	1673.00
0.1	1657.00	1665.00	1665.00	1672.80	1673.20
1	1656.75	1664.63	1664.88	1670.78	1674.73
2	1656.03	1663.58	1664.56	1668.15	1676.05
3	1654.92	1662.04	1664.02	1665.34	1677.19

[a]Values in this row are the theoretical values at $J=0$.

TABLE III. $D2$ soliton energies with $\hbar\omega_0 = 1665\ \mathrm{cm}^{-1}$.

Set	$\hbar\omega_a$ (cm^{-1})	$\overline{\chi}$ (cm^{-1})	J (cm^{-1})	$\hbar\eta$ (cm^{-1})	$J/\hbar\eta$	n	E_S (cm^{-1})
			Class 1: Small J regime				
1	100	5	1	0.500	2.000	8	1662.132
2	100	7	1	0.980	1.020	5	1660.587
3	100	8	1	1.280	0.781	5	1659.497
4	100	9	1	1.620	0.617	4	1658.215
5	100	10	1	2.000	0.500	4	1656.752
6	95	10	1	2.105	0.475	4	1656.341
7	90	10	1	2.222	0.450	4	1655.886
8	85	10	1	2.353	0.425	4	1655.377
9	100	5	2	0.500	4.000	12	1660.448
10	100	7	2	0.980	2.041	8	1659.318
11	100	10	2	2.000	1.000	5	1656.032
12	95	10	2	2.105	0.950	5	1655.655
13	90	10	2	2.222	0.900	5	1655.233
			Class 2: Alpha-helix regime				
14	88	10	7.8	2.273	3.436	11	1646.601
15	88	11	7.8	2.750	2.833	9	1645.548
16	70	10	7.8	2.857	2.732	9	1645.297
17	60	10	7.8	3.333	2.342	8	1644.127
18	50	10	7.8	4.000	1.949	7	1642.349
19	50	11	7.8	4.840	1.610	7	1639.898

width of the localized state in the continuum model [5]. In Fig. 4 we plot this parameter versus the values in column n of Table III. We find that this parameter tracks with the size of the localized state for the discrete chain. We note also the tendency for each curve in Fig. 4 to drop away from the diagonal as E_S decreases. This behavior tracks with the narrowing of the state as found by examining column n in Table III and further agrees with the contention that broader localized states will trend toward the continuum model.

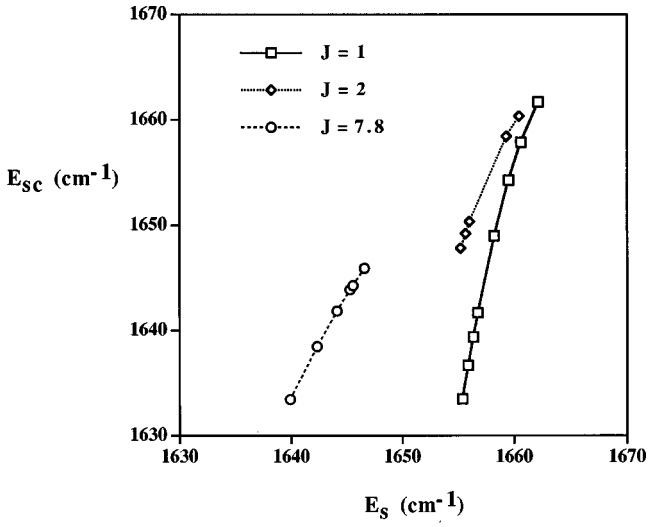

FIG. 3. Correlation plot for discrete chain soliton energy E_S vs continuum model energy E_{SC}.

IV. $D1$ ANSATZ

The $D1$ Davydov ansatz allows for site dependence of the parameters s_k in Eq. (13) and is considered a more general form for dressing the vibron operator c_m [15,19]. In terms of a $D1$ soliton creation operator the ansatz is given by [14]

TABLE IV. Comparison of continuum envelope with discretized envelope.

n	$\left(\frac{2\hbar\eta}{J}\right)^{1/2}\mathrm{sech}\left(\frac{4\hbar\eta}{J}n\right)$	a_{ns}
	Set 9 $J/\hbar\eta = 4.000$	
0	0.7071	0.6327
1	0.4582	0.4753
2	0.1880	0.2436
3	0.0702	0.1089
4	0.0259	0.0472
5	0.0095	0.0203
6	0.0035	0.0087
7	0.0013	0.0038
8	0.0005	0.0016
9	0.0002	0.0007
10	0.0001	0.0003
11	0.0	0.0001
	Set 5 $J/\hbar\eta = 0.500$	
0	2.0000	0.9845
1	0.0013	0.1240
2	0.0	0.0078

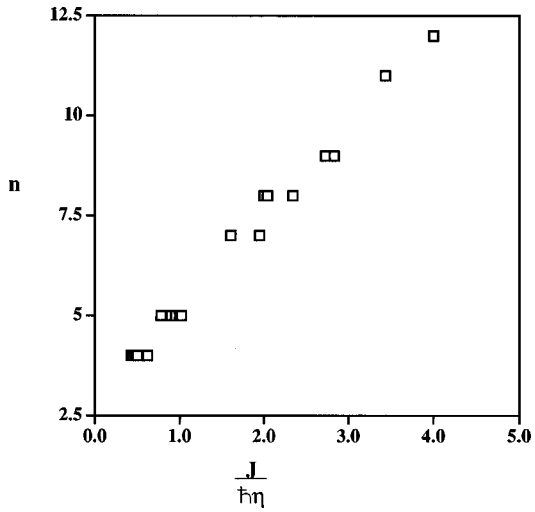

FIG. 4. Comparison of the parameter $J/\hbar\eta$ with the value n for which a_{ns} first drops below 10^{-4}.

$$A_s^\dagger = \sum_m a_{ms} c_m^\dagger \exp\left[\sum_k (s_k^{(m)} a_k - s_k^{(m)*} a_k^\dagger) \right]. \tag{41}$$

To make use of this definition, we first obtain the expectation value of the Hamiltonian in Eq. (6) using a state formed by operation of the creation operator in Eq. (41) on the vacuum state. Assuming only cyclic boundary conditions given by

$$s_k^{(N+1)} = s_k^{(-N)} \tag{42}$$

and

$$a_{N+1,\nu} = a_{-N,\nu}, \tag{43}$$

where $s_k^{(m)}$ is allowed to be complex and $a_{m\nu}$ is taken to be real, we obtain

$$\begin{aligned} E_s = \hbar\omega_0 \sum_{m=-N}^{N} a_{ms}^2 + \sum_{m=-N}^{N} a_{ms}^2 \sum_{k=-N}^{N} (\hbar\omega_k s_k^{(m)} s_k^{(m)*} \\ + \chi_k^{(m)} s_k^{(m)*} + s_k^{(m)} \chi_k^{(m)*}) - 2J \sum_{m=-N}^{N} a_{ms} a_{m+1,s} \\ \times \exp\left[-\frac{1}{2} \sum_{k=-N}^{N} (s_k^{(m)} - s_k^{(m+1)})(s_k^{(m)*} - s_k^{(m+1)*}) \right] \\ \times \cos\left[\sum_{k=-N}^{N} ({}^R s_k^{(m)} {}^I s_k^{(m+1)} - {}^I s_k^{(m)} {}^R s_k^{(m+1)}) \right]. \end{aligned} \tag{44}$$

The superscripts R and I indicate real and imaginary parts. We have dropped zero-point energy terms and the phonon energy from Eq. (44). We have not included a thermal average of the phonon bath, which is sometimes done (so-called thermalized Hamiltonian) [5] since we agree with Schweitzer [11] that this procedure is contrary to normal practice in quantum statistical mechanics. Such an average adds the factor $\coth(\hbar\beta\omega_k/2)$ to the exponential in the term which depends on J. We include the effect of temperature in a separate paper by examining the behavior of relevant time correlation functions where appropriate quantum statistical averages have been taken in a rigorous, systematic manner.

To properly use Eq. (44), there are some technical points related to the $k=0$ terms. We first require that the factors $s_0^{(n)}$ be independent of the site label n. This is a minor restriction on the wave function ansatz, which keeps the exponential factor in Eq. (44) from misbehaving. We next scale the resulting factor such that $s_0 = (\sigma_0/\omega_0)\overline{s_0}$. Using Eq. (12), this permits us to express the $k=0$ terms in Eq. (44) in terms of the parameter η. In the work below we treat $\overline{s_0}$ as the variational parameter for $k=0$ terms. It is allowed to be a complex number.

With the technical points for $k=0$ in hand, we have minimized the energy expression in Eq. (44) using the simulated annealing procedure in Appendix A by independently varying the parameters a_{ms}, ${}^R s_k^{(m)}$, and ${}^I s_k^{(m)}$ subject to the normalization constraint $\sum_{m=-N}^{N} a_{ms}^2 = 1$. We have changed both N, the size of the cyclic chain, and the initial starting point. As starting points for the annealing, we have chosen (1) the $D2$ values for the parameters as described in Secs. II and III, and (2) the values for a uniform polaron, namely,

$$a_{ms} = \frac{1}{\sqrt{2N+1}} \tag{45}$$

and

$$s_k^{(m)} = -\frac{\chi_k^{(m)}}{\hbar\omega_k}. \tag{46}$$

We point out that for N sufficiently large, the localized $D2$ soliton is unaffected to a high degree of numerical accuracy by the choice of cyclic as opposed to truncated chain boundaries. We find for all cases studied including $N=1-5$, 10, 21 with Hamiltonian parameters specified by set 14 in Table III that a common minimum energy state is always achieved and that the variational parameters are given by

$$a_{ms} = \frac{1}{\sqrt{2N+1}} \tag{47}$$

and

$$s_k^{(m)} = -\frac{\lambda_k}{\hbar\omega_k} \chi_k^{(m)} \tag{48}$$

where λ_k is essentially the only free variational parameter and is real and even in k. This seems like a remarkable result considering that a large number of freely varying parameters converge to this simple form. However, comparing with Eqs. (45) and (46), we see that the minimum energy state for the $D1$ ansatz is a modified uniform polaron state as required by translational symmetry for the eigenstates of the full Hamiltonian [20], and is not a localized state as proposed by Davydov [14]. It is evident from Eq. (44) that E_s cannot be minimized with respect to a_{ms} under the constraints of normalization for the a_{ms} in Eq. (23) and translational symmetry unless the exponential factors become independent of lattice site number n. This requirement leads directly to Eq. (48).

In analogy with Eq. (19) for the $D2$ case, it is useful to set up a similar Hamiltonian for the $D1$ case in order to estab-

lish a Hamiltonian H_0 and a spectrum of oscillator energies. To accomplish this transformation of the Davydov Hamiltonian in Eq. (6), we define

$$f_n=\sum_k \frac{\lambda_k}{\hbar\omega_k}(\chi_k^{(n)}a_k-\chi_k^{(n)*}a_k^\dagger), \tag{49}$$

$$U^\dagger=\exp\left(\sum_m c_m^\dagger c_m f_m\right), \tag{50}$$

$$d_m=Uc_mU^\dagger=c_m e^{f_m}, \tag{51}$$

and

$$b_k=Ua_kU^\dagger=a_k+\sum_m s_k^{(m)*}c_m^\dagger c_m, \tag{52}$$

with $c_m^\dagger c_m=d_m^\dagger d_m$. It can be shown that

$$[f_n,f_m]=0 \tag{53}$$

and

$$\langle e^{f_n-f_{n+1}}\rangle_v=\langle e^{f_{n+1}-f_n}\rangle_v =\exp\left(-8\sum_k \frac{\lambda_k^2\sigma_k^2}{\hbar^2\omega_k^2}\sin^2\frac{\pi k}{2N+1}\right), \tag{54}$$

where the expectation value is taken with respect to the vacuum state denoted by subscript v. With these definitions we find that

$$\begin{aligned}H=H_0&+\sum_k \hbar\omega_k b_k^\dagger b_k-J\sum_n [(e^{-f_n+f_{n+1}}\\&-\langle e^{-f_n+f_{n+1}}\rangle_v)d_n^\dagger d_{n+1}\\&+(e^{-f_{n+1}+f_n}-\langle e^{-f_{n+1}+f_n}\rangle_v)d_{n+1}^\dagger d_n]\\&+\sum_{kn}[(\lambda_k-1)\chi_k^{(n)}b_k+(\lambda_k-1)\chi_k^{(n)*}b_k^\dagger]d_n^\dagger d_n\\&+\sum_{nm}\left[\sum_k \chi_k^{(m)}\chi_k^{(n)*}\left(\frac{\lambda_k^2-2\lambda_k}{\hbar\omega_k}\right)\right]d_m^\dagger d_n^\dagger d_m d_n\end{aligned} \tag{55}$$

and

$$H_0=\sum_n\left\{\left[\hbar\omega_0+\sum_k \frac{\sigma_k^2}{\hbar\omega_k}(\lambda_k^2-2\lambda_k)\right]\times d_n^\dagger d_n-\overline{J}(d_n^\dagger d_{n+1}+d_{n+1}^\dagger d_n)\right\}, \tag{56}$$

with

$$\overline{J}=J\exp\left(-8\sum_k \frac{\lambda_k^2\sigma_k^2}{\hbar^2\omega_k^2}\sin^2\frac{\pi k}{2N+1}\right). \tag{57}$$

Diagonalization of H_0 produces the $D1$ spectrum of oscillator energies when λ_k is chosen to minimize the lowest energy value. Note that the phonon-vibron interaction term in Eq. (55) vanishes for $\lambda_k=1$. We further note that the form of the expectation value in Eq. (44) requires one for completeness to set up the Hamiltonian in Eq. (55) with terms involving the vacuum expectation value in Eq. (54). These interaction terms, although small in magnitude, should not be ignored when dynamics is considered.

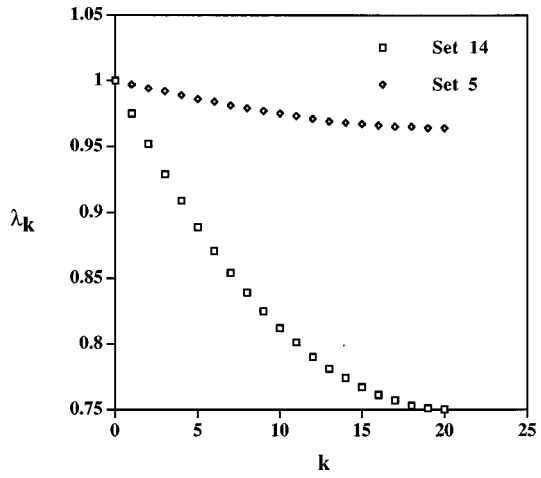

FIG. 5. Plots of λ_k values for sets 5 and 14 with $N=20$.

As a concrete example of the results obtained for $D1$ minimization, we show in Fig. 1 a comparison of the oscillator energy spectrum E_ν obtained by $D1$ and $D2$ minimization using set 14 with $N=20$. The $D1$ spectrum clearly lies below the $D2$ spectrum and there is not a gap separating the lowest-energy oscillator from higher-energy ones within the limits of the finite chain computation. Similar results for set 5 are shown in Fig. 2. Plots of λ_k values for sets 5 and 14 are given in Fig. 5.

Since the $D1$ ansatz as described by Eqs. (47) and (48) is the lowest energy solution, we consider next the issue of whether the $D2$ state is at least metastable with respect to changes in the parameters a_{ns} and $s_k^{(n)}$. To accomplish this task, we set all a_{ns} and $s_k^{(n)}$ values equal to their $D2$ values except for one $s_k^{(n)}$, which is specified as $s_i^{(p)}=s_i^{D2}+{}^R\sigma_i^{(p)}$ where ${}^R\sigma_i^{(p)}$ is an infinitesimal, real change. Substitution into Eq. (44) yields to lowest order in ${}^R\sigma_i^{(p)}$ the result

$$E_s=E_s^{D2}+a_{ps}^{D2}\left[\chi_i^{(p)}+\chi_i^{(p)*}-2\sum_{m=-N}^{N}a_{ms}^{D2}\chi_i^{(m)}\right]{}^R\sigma_i^{(p)}, \tag{58}$$

where the superscript $D2$ indicates $D2$ soliton values. The coefficient of ${}^R\sigma_i^{(p)}$ is clearly a real number and thus ${}^R\sigma_i^{(p)}$ can be chosen to have the appropriate sign to lower the energy E_s relative to E_s^{D2}. Therefore, the $D2$-soliton energy E_s^{D2} is not a metastable point in the space of a_{ns} and $s_k^{(n)}$ since infinitesimal changes in one of the $s_k^{(n)}$ can lower the energy.

To further pursue this point regarding the choice of the wave function ansatz or creation operator and the energy surface E_s, it is useful to consider the modified $D1$ ansatz due to Brown and Ivic [15]. We call this case the BI ansatz and it is given by

$$s_k^{(n)}=s_k-\delta\frac{\chi_k^{(n)}}{\hbar\omega_k}, \tag{59}$$

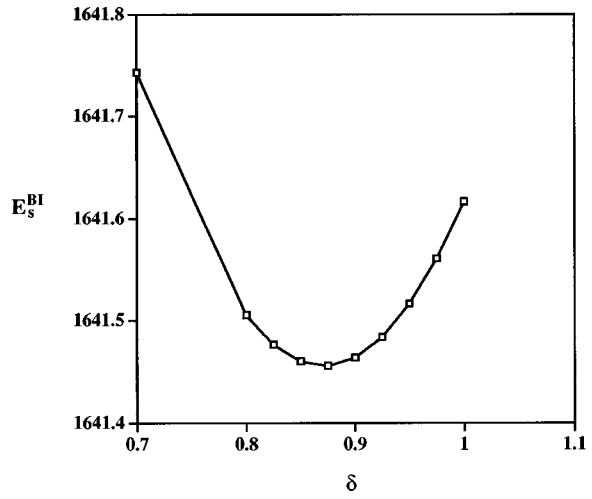

FIG. 6. E_s^{BI} as a function of δ for set 14.

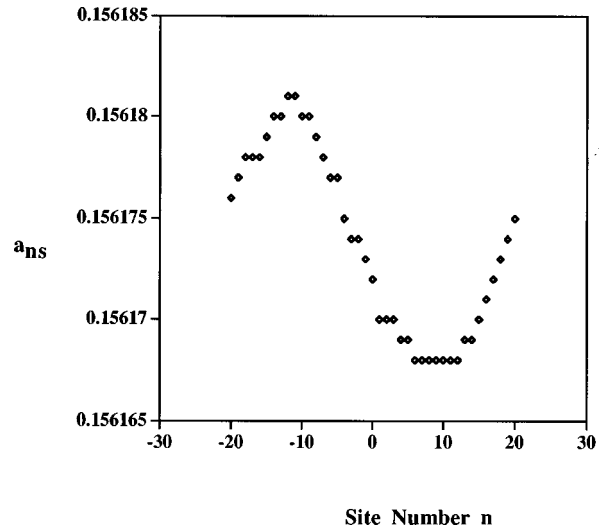

FIG. 7. Site amplitudes a_{ns} for BI computation of set 14 at $\delta=0.875$.

where δ is a variational parameter. This choice for $s_k^{(n)}$ represents a constraint upon the form of $s_k^{(n)}$ as compared to the full $D1$ minimization considered above and is expected to produce a higher energy. As pointed out by Brown and Ivic [15], this form allows one to move from the $D2$ soliton ($\delta=0$) to the standard uniform polaron ($\delta=1$). Substitution of Eq. (59) into Eq. (44) with minimization of s_k yields

$$E_s^{\mathrm{BI}}=[\hbar\omega_0+(\delta^2-2\delta)4\hbar\eta]\sum_{n=-N}^{N}a_{ns}^2+(\delta-1)^2 4\hbar\eta\sum_{n=-N}^{N}(a_{ns}^4+a_{ns}^2a_{n+1,s}^2)-2J_{\mathrm{BI}}\sum_{n=-N}^{N}(a_{ns}a_{n+1,s}), \tag{60}$$

with

$$J_{\mathrm{BI}}=J\exp\left(-8\delta^2\sum_{k=-N}^{N}\frac{\sigma_k^2}{\hbar^2\omega_k^2}\sin^2\frac{\pi k}{2N+1}\right) \tag{61}$$

and

$$a_{N+1,s}=a_{-N,s} \tag{62}$$

when cyclic boundary conditions are imposed. For fixed δ we have used the simulated annealing algorithm in Appendix A to find a_{ns} and E_s^{BI}. A plot of E_s^{BI} as a function of δ is given in Fig. 6 using set 14 parameters. The corresponding a_{ns} values for $\delta=0.875$ are shown in Fig. 7. We find from Fig. 6 that there is a minimum in E_s^{BI} near $\delta=0.875$; however, the curve for E_s^{BI} lies above the $D1$ minimization value of $E_s=1641.415\,267\ \mathrm{cm}^{-1}$. This is as expected since the BI ansatz is constrained relative to $D1$. Brown and Ivic make the point that the energy difference between E_s^{BI} at $\delta=0.875$ and E_s^{BI} at $\delta=1.0$, the standard uniform polaron limit, represents an energy gap that can sustain the localized structure shown in Fig. 7. We note that the location of the center of the soliton in Fig. 7 at about $n=-11$ arises from the nature of the random walk used for convergence and the fact that a_{ns} deviates only slightly from the uniform value of 0.156 1738 at $N=20$. The center of the soliton freezes out randomly. The values of a_{ns} are converged to within $\pm10^{-6}$, which accounts for the small amount of noise in the plot.

From our perspective we find that full minimization of the $D1$ ansatz without constraints leads to the loss of localization and the energy gap through the formation of the modified uniform polaron solution of Eqs. (47) and (48). This is consistent with the requirement of translational symmetry for the eigenstates. Although these time-independent $D1/D2$ results suggest that a $D2$ soliton will be unstable, it is possible that the $D2$ state, once created, can exist coherently for a period of time via bottlenecking or related effects. We address these lifetime issues in a separate paper.

V. SUMMARY

Several decades after its introduction, the existence of the Davydov soliton in molecular chains continues to be a question. As pointed out by Cottingham and Schweitzer [9–11], the key to proving its existence lies in correct and appropriate application of quantum statistical mechanical principles to the problem. A first step in this regard is the partial diagonalization principle introduced by Eremko, Gaididei, and Vakhnenko for the continuum limit case [8]. This approach allows one to explicitly display the soliton as a creation operator in the Hamiltonian. The next step is to remove the restriction to the continuum case and carry out partial diagonalization on a molecular chain. We have carried out this step herein for the $D2$ soliton case by transforming the standard Davydov Hamiltonian in Eq. (1) into the form in Eq. (33), which explicitly includes the soliton, self-localized state. For a chain of length $2N+1$ this transformation is rigorous and involves no approximations other than numerical diagonalization of a matrix.

The transformation from Eq. (1) to Eq. (33) involves the use of an approach for computing the soliton envelope, a_{ns}; namely, simulated annealing. This procedure allows for accurate and rapid computation of a_{ns} for a zero momentum Davydov soliton located at the center of the chain on site 0.

We argue that the Hamiltonian in Eq. (33) is the proper starting point for an analysis of the Davydov problem in the context of the standard $D2$ Davydov soliton.

The creation operator for the soliton state in Eq. (13) uses the standard $D2$ form for the Davydov soliton and it can be argued that this is not the best form. We address this point by examining the more general form known as the $D1$ ansatz in Eq. (41). This choice leads to the energy expression in Eq. (44), which is to be minimized. Using the simulated annealing approach that allows for arbitrary variations of all the ansatz parameters, we have found that the minimum solution always turns out to be a modified uniform polaron solution with the ansatz parameters given by Eqs. (47) and (48). We believe this to be a result that potentially has application to other condensed matter problems involving similar polaron-like transformations. In obtaining this result we have made no symmetry assumptions regarding the ansatz parameters other than the cyclic condition that the endpoints of the chain (labeled -N and N) are coupled. This condition is reflected in Eqs. (42) and (43). We have shown further that the $D2$ soliton energy is not metastable and can be lowered by infinitesimal changes in the parameter $s_k^{(n)}$. The Brown-Ivic modified $D1$ ansatz, a constrained form of the full $D1$ ansatz, is found to have an energy above the full $D1$ solution (modified uniform polaron) but below the standard uniform polaron solution. From our viewpoint of using the full $D1$ case, the soliton and polaron perspectives merge to form a modified uniform polaron solution as described by Eqs. (47) and (48).

Although the $D2$ soliton that arises from a restricted form of the $D1$ ansatz is higher in energy than the $D1$ case, it is possible that, if formed, it could persist as a coherent state. The gap shown in Fig. 1 between the localized, lowest-energy oscillator energy ($D2$ soliton) and the other levels enhances this viewpoint. On the other hand Cottingham and Schweitzer have shown using continuum partial diagonalization and second-order perturbation theory that the decay time is very short (less than a picosecond) for set 14 [9–11]. However, a serious issue in this case is the use of the continuum approximation, simple perturbation theory, and the meaning of the decay time computed. The general problem resides in the question of how one carries out quantum dynamics for condensed matter problems. In a separate paper we examine this problem in the context of Davydov $D2$ solitons using the partially diagonalized, discrete molecular chain Hamiltonian in Eq. (33).

We conclude by observing that the $D2$ and $D1$ creation operators in Eqs. (13) and (41) insert one quanta into the vibron modes. Kerr and Lomdahl [21,22], following a suggestion by one of us (AMC), have examined the case for multiquanta creation operators. To date they have found that increasing the number of quanta does not increase the stability of the soliton.

ACKNOWLEDGMENTS

We thank the Robert A. Welch Foundation (Grant Nos. Y-1234 and Y-1303) for their support of this research.

APPENDIX A: SIMULATED ANNEALING SOLUTION FOR ENVELOPE AMPLITUDES

To obtain a set of envelope amplitudes, a_{ns}, which minimize the energy in Eq. (32), we use a simulated annealing algorithm. Since the expected localized solution has zero momentum, we start by setting $a_{ns}=\delta_{n0}$; that is, we localize the envelope at site 0 in the middle of the chain. We then carry out a Metropolis Monte Carlo walk as follows: we select a new value for the coefficients according to the rule

$$a_{ns}^{(\mathrm{new})}=a_{ns}^{(\mathrm{old})}+\delta(R-\tfrac{1}{2}), \tag{A1}$$

where δ is a jump distance and R is a uniform random number between 0 and 1. We next uniformly scale the new values to maintain the normalization

$$1=\sum_n (a_{ns}^{(\mathrm{new})})^2. \tag{A2}$$

We compute a new energy, $\hbar E_s^{(\mathrm{new})}$, from Eq. (32) and a test function e^x where

$$x=\frac{E_s^{(\mathrm{old})}-E_s^{(\mathrm{new})}}{T_a}, \tag{A3}$$

where T_a is an annealing temperature. If the test function is greater than one, we accept the move. If the test function is less than one, we compare with R and accept the move if greater than the random number. The parameters δ and T_a are chosen and varied interactively until convergence is obtained on E_s. We find that the process goes very quickly and one can obtain the envelope amplitudes a_{ns} to any desired accuracy.

APPENDIX B: PARTIAL DIAGONALIZATION

In this appendix we examine the partial diagonalization procedure of Eremko, Gaididei, and Vakhnenko [8] as pursued by Cottingham and Schweitzer [9–11] in terms of a discrete chain using the notation of Sec. II. We begin by carrying out a linear shift of the phonon modes such that

$$b_k=a_k-f_k, \tag{B1}$$

where f_k is a c number. Note the difference with Eq. (16) where the shift contains the occupation number operator in the high-frequency vibrational modes. It is at this juncture that we differ with the previous partial diagonalization process. Using Eq. (B1), we find that the Hamiltonian is transformed to

$$H=H_0+\sum_{k=-N}^{N}\hbar\omega_k b_k^\dagger b_k+\sum_{k=-N}^{N}\hbar\omega_k(f_k^* b_k+b_k^\dagger f_k)$$
$$-\sum_{k=-N}^{N}\sum_{n=-N}^{N} c_n^\dagger c_n(\chi_k^{(n)} b_k+\chi_k^{(n)*} b_k^\dagger), \tag{B2}$$

with

$$H_0=\sum_{n=-N}^{N}\{\varepsilon_n c_n^\dagger c_n-J(c_n^\dagger c_{n+1}+c_{n+1}^\dagger c_n)\}+W, \tag{B3}$$

$$W=\sum_{k=-N}^{N}\hbar\omega_k f_k^* f_k, \tag{B4}$$

and

$$\varepsilon_n=\hbar\omega_0-\sum_{k=-N}^{N}(\chi_k^{(n)}f_k+\chi_k^{(n)*}f_k^*). \tag{B5}$$

This form for the Hamiltonian matches the form discussed by Cottingham and Schweitzer [10].

We next diagonalize H_0 by the transformation

$$c_n=\sum_{\nu=-N}^{N}a_{n\nu}A_\nu \tag{B6}$$

to give

$$H_0=\sum_{\nu=-N}^{N}E_\nu A_\nu^\dagger A_\nu+W \tag{B7}$$

and choose the shift to have the form

$$f_k=\sum_{m=-N}^{N}a_{ms}^2\frac{\chi_k^{(m)*}}{\hbar\omega_k}. \tag{B8}$$

With this choice one can show that

$$E_s+W=\hbar\omega_0-2\hbar\eta\sum_n a_{ns}^2(2a_{ns}^2+a_{n+1,s}^2+a_{n-1,s}^2)$$

$$-2J\sum_n a_{ns}a_{n+1,s}, \tag{B9}$$

which is the standard form for the soliton energy in Eq. (32).

The essential difference between our approach to partial diagonalization and that chosen by previous authors is that we use the dressed operators D_n as opposed to the bare operators c_n. This permits a more compact form for the Hamiltonian as shown in Eq. (33) and removes remaining linear shift terms for the phonon operators as found in Eq. (B2).

[1] A. S. Davydov, J. Theor. Biol. **38**, 559 (1973).

[2] A. S. Davydov and N. I. Kislukha, Phys. Status Solidi B **59**, 465 (1973).

[3] *Davydov's Soliton Revisited*, edited by P. L. Christiansen and A. C. Scott (Plenum, New York, 1990).

[4] A. S. Davydov, *Solitons in Molecular Systems*, 2nd ed. (Reidel, Dordrecht, 1991).

[5] A. Scott, Phys. Rep. **217**, 1 (1992).

[6] G. Careri, U. Buontempo, F. Carta, E. Gratton, and A. C. Scott, Phys. Rev. Lett. **51**, 304 (1983).

[7] G. Careri, U. Buontempo, F. Galluzzi, A. C. Scott, E. Gratton, and E. Shyamsunder, Phys. Rev. B **30**, 4689 (1984).

[8] A. A. Eremko, Y. B. Gaididei, and A. A. Vakhnenko, Phys. Status Solidi B **127**, 703 (1985).

[9] J. P. Cottingham and J. W. Schweitzer, Phys. Rev. Lett. **62**, 1792 (1989).

[10] J. W. Schweitzer and J. P. Cottingham, in *Davydov's Soliton Revisited* (Ref. [3]), p. 285.

[11] J. W. Schweitzer, Phys. Rev. A **45**, 8914 (1992).

[12] A. S. Davydov, Phys. Scr. **20**, 387 (1979).

[13] See *Davydov's Soliton Revisited* (Ref. [3]), Sec. II.

[14] A. S. Davydov, Zh. Eksp. Teor. Fiz. **78**, 789 (1980) [Sov. Phys. JETP **51**, 397 (1980)].

[15] D. W. Brown and Z. Ivic, Phys. Rev. B **40**, 9876 (1989).

[16] G. Venzl and S. F. Fischer, J. Chem. Phys. **81**, 6090 (1984).

[17] W. H. Press, B. P. Flannery, S. A. Teukolsky, and W. T. Vetterling, *Numerical Recipes* (Cambridge University Press, Cambridge, 1986), Sec. 11.1.

[18] L. Brizhik, Y. B. Gaididei, A. A. Vakhnenko, and V. A. Vakhnenko, Phys. Status Solidi B **146**, 605 (1988).

[19] W. Former, J. Phys.: Condens. Matter **5**, 3897 (1993). See Appendix 3.

[20] D. Emin, Adv. Phys. **22**, 57 (1973).

[21] W. C. Kerr and P. S. Lomdahl, in *Davydov's Soliton Revisited* (Ref. [3]), p. 23.

[22] P. S. Lomdahl and W. C. Kerr, in *Davydov's Soliton Revisited* (Ref. [3]), p. 259.